Materials Chemistry and Physics 153 (2015) 316–322

Contents lists available at ScienceDirect

Materials Chemistry and Physics

journal homepage: www.elsevier.com/locate/matchemphys

Synthesis of spherical bismuth nanoparticles by two-step heating of tetraethylene glycol containing solid bismuth(III) carbonates

Ji Hwan Kim, Jong-Hyun Lee*

Department of Materials Science & Engineering, Seoul National University of Science & Technology, 232 Gongneung-ro, Nowon-gu, Seoul 139-743, Republic of Korea

HIGHLIGHTS

- Synthesis of nano-sized Bi particles was implemented using insoluble solid precursor.
- The bismuth particles exhibited excellent sphericity and dispersity.
- Synthesis mechanism was discussed.
- Deviation in size was discussed by varying the main process parameters.
- TEM study on as-synthesized particles was performed.

ARTICLE INFO

Article history:
Received 30 August 2014
Received in revised form
18 December 2014
Accepted 3 January 2015
Available online 7 January 2015

Keywords:
Metals
Chemical synthesis
X-ray reflectivity
Phase transitions

ABSTRACT

Synthesis of nano-sized spherical bismuth particles was implemented by a novel polyol method using insoluble solid Bi(III) subcarbonate particles. The Bi(III) subcarbonate precursor was directly reduced and gradually transformed to Bi nanoparticles (NPs) from 240 °C with an increase of temperature during a two-step heating process to 300 °C. Although some Bi(III) subcarbonate platelets were not transformed completely to the Bi NPs even after heating to 300 °C, complete removal of the Bi(III) subcarbonate platelets and the enhanced sphericity of the synthesized Bi NPs were accomplished with a holding step at the target temperature for 35 min. The Bi NPs were synthesized under optimized conditions, including preheating at 200 °C for 1 h. The Bi NPs had an average diameter of approximately 60 nm, and they exhibited excellent sphericity and dispersity.

1. Introduction

Bismuth is a nonferrous rare metal that is used in medicines, cosmetics, ceramic glazes, pigments, and lubricants [1]. In metal industries, Bi has been used in galvanizing and as a nontoxic substitute for lead in solder alloys [2–4]. Also, research on monodispersed spherical Bi particles used as photonic crystals has been conducted [5]. More recently, it was suggested as a material for novel electronic applications mainly due to its high anisotropic electronic behavior, high intrinsic electron mobility, and low conduction electron effective mass [6].

Despite the potential increase in the use of finely dispersed Bi nanoparticles (NPs) in all these technology fields, there have been few reports of an effective and economic preparation method of Bi NPs using a wet chemical reaction with polyol [1,7,8]. Although Bi has been synthesized as colloidal particles by some chemical methods, most of the synthesized particles were either irregular in terms of their size or shape or had an average diameter greater than 100 nm [9–12]. Moreover, the synthesis mechanism in the chemical methods was either ambiguous or not discussed in detail.

In this work, we prepared sub-100 nm Bi NPs with excellent sphericity via a simple and convenient novel polyol synthesis. The Bi precursor used was Bi(III) carbonate basic. We used tetraethylene glycol and polyvinyl pyrrolidone (PVP) as a polyol solvent and a capping agent, respectively. We elucidate the synthesis mechanism of the Bi NPs through scrupulous SEM observation, and we control the average particle size and deviation in size by varying the main process parameters.

* Corresponding author.
E-mail address: pljh@snut.ac.kr (J.-H. Lee).

http://dx.doi.org/10.1016/j.matchemphys.2015.01.019
0254-0584/

2. Experimental procedures

The typical synthesis procedure of Bi NPs was as follows. 1.275 g of Bi(III) subcarbonate basic powder [$(BiO)_2CO_3$, 80–82% Bi basis, Fluka] as a precursor was added to 25 mL of tetraethylene glycol [TEG, $HO(CH_2CH_2O)_3CH_2CH_2OH$, 99%, Aldrich]. The mixture was stirred until the precursor powder was well dispersed in the solvent. Then, 7.3 g of polyvinyl pyrrolidone (PVP, MW = 10,000, Sigma–Aldrich) was put into a 500 mL reactor containing 75 mL TEG. The reactor with a condensation system was preheated to the target preheating temperature (typical preheating temperature: 200 °C) using a heating mantle. Then, 25 mL of the Bi(III) subcarbonate mixture was poured into 75 mL of the heated PVP mixture. As a result, the initial concentration of Bi(III) subcarbonate was 25 mM. After the mixing, the mixture was maintained at the target preheating temperature for 1 h in air. After the preheating, the mixture was heated to 300 °C and held for different lengths of time. Finally, the heated mixture was cooled rapidly by pouring 500 mL of methanol (MeOH, 99.8%, Duksan Pure Chemicals) into the reactor. The cooling process reduced the possibility of aggregation or coalescence of the Bi NPs, eventually decreasing the irregularity of particle shape and the deviation in particle size. The abovementioned heating procedures are summarized in Fig. 1. After cooling, the morphology and crystalline phases of as-synthesized particles were observed by high-resolution transmission electron microscopy (HRTEM, Tecnai 20, FEI Co.). The sample for analysis was prepared by adding a few drops of the solution containing the particles to a carbon-coated copper grid.

The synthesized gray particles in the solution were centrifuged and collected. The particles were washed repeatedly with MeOH during the centrifugation and dried in a desiccator at room temperature for further characterization. The composition and shape of the as-synthesized products were characterized using power X-ray diffraction (XRD, X'pert MPD, Philips) and scanning electron microscopy (SEM, VEGA3, TESCAN).

3. Results and discussion

Fig. 2 shows the SEM images of the transition from Bi(III) subcarbonate to spherical Bi nanoparticles during the two-step heating process, which consisted of preheating and a second heating to 300 °C. All images except that shown in Fig. 2a were taken after the mixtures were held at each temperature for 5 min and cooled to room temperature. Fig. 2a is a sample obtained after holding at 200 °C for l h, and the platelet particles are Bi(III) subcarbonate precursor powders. As can be seen, no apparent alteration in the Bi(III) subcarbonate powders was observed even after l h at 200 °C. However, some spherical NPs were formed, as observed in Fig. 2b, after heating to 240 °C, and the spherical NPs were identified as Bi-phase particles, which matches the results of Fig. 3 The number of spherical Bi NPs increased with an increase in the temperature of the medium to 300 °C. In other words, the Bi(III) subcarbonate platelets transformed increasingly to spherical Bi NPs with increasing reaction temperature. However, some Bi(III) subcarbonate platelets did not transform to Bi NPs; they remained even after heating to 300 °C.

Interestingly, the spherical Bi NPs grew from the edge or basal surface of the plate-like Bi(III) subcarbonate particles. As a result, holes or concave faces were observed in the edges or basal surfaces of the Bi(III) subcarbonate platelets. The red broken lines and red arrows in the magnified SEM images of Fig. 4 indicate these phenomena. The Bi(III) subcarbonate platelet precursor did not dissolve in TEG. Thus, it is judged that electrons participating in reducing the precursor particles to Bi NPs are directly supplied from the TEG solvent to the surfaces of the plate-like Bi(III) subcarbonate. The electrons may have originated from acetaldehyde by the thermal degradation of TEG as follows. TEG [$HO(CH_2CH_2O)_3CH_2$-CH_2OH] can be decomposed to acetaldehyde (CH_3CHO), diethyl ether ($C_2H_5OC_2H_5$), and oxygen during heating (Equation (1)) [13–15]. The oxidation of acetaldehyde donates electrons to the Bi(III) subcarbonate, together with hydrogen cations, and Bi ions in the Bi(III) subcarbonate are reduced to Bi atoms while the surfaces of the Bi(III) subcarbonate receive the electrons (Equation (2)) [13,16]. After the donation of electrons, acetaldehyde is converted into diacetyl.

$$HO(CH_2CH_2O)_3CH_2CH_2OH \rightarrow 2CH_3CHO + C_2H_5OC_2H_5 + O_2 \quad (1)$$

$$6CH_3CO\cdot + 6H^+ + 2Bi^{3+} \rightarrow 2Bi + 6H^+ + 3CH_3COCOCH_3 \quad (2)$$

These reaction mechanisms may explain well the formation of spherical Bi NP initiates on the local surfaces of solid Bi(III) carbonate particles. Once pure Bi NPs are formed, the shape of the Bi NPs will begin to take a spherical shape in order to reduce their surface energy, becoming almost perfectly spherical by melting when the heating temperature surpasses the melting point of Bi (272 °C). While the medium is cooled rapidly to room temperature, the molten spherical Bi NPs solidify while maintaining their shape. It is also estimated that heat energy or electron donation are not enough to completely reduce Bi(III) subcarbonate particles to spherical Bi NPs until the reaction temperature is increased to 300 °C.

Fig. 3 shows XRD patterns of the reduction of Bi(III) subcarbonate with increasing heating temperature. During the preheating at 200 °C for 1 h, it was confirmed that the phase transformation from Bi(III) subcarbonate to Bi NPs was minimal. However, the peaks of Bi(III) subcarbonate gradually disappeared with the gradual increase of Bi peaks during the second step of heating to 300 °C, indicating the gradual reduction of Bi(III) subcarbonate. With increasing temperature of the medium in the range from 270 °C to 300 °C, the Bi peaks abruptly became much stronger. At the end of the reaction corresponding to 300 °C, the peaks of Bi(III) subcarbonate are minimal and the Bi peaks remain at the highest intensity. These results agree well with the images shown in Fig. 2. The synthesis mechanism of Bi NPs from Bi(III) subcarbonate can be summarized as shown in Fig. 5.

To enhance the sphericity of the Bi NPs, the holding time at 300 °C was increased to 60 min. Fig. 6 shows the SEM images of the Bi NPs synthesized with different holding times at 300 °C. The Bi NPs synthesized with a holding time of 35 min exhibited significantly enhanced sphericity in comparison with those synthesized

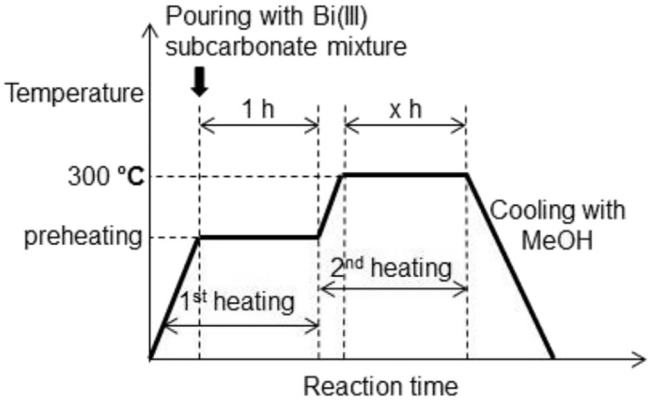

Fig. 1. Heating procedures used to fabricate sub-100 nm spherical Bi NPs.

with a holding time of 5 min (Fig. 2h). This means that the transition from Bi(III) subcarbonate to Bi NPs is a time-consuming process. However, additional holding induced the size increase of Bi NPs, as observed in Fig. 6b and c. 300 °C is a high temperature, such that the stability of PVP cannot be guaranteed [17,18]. Hence, the long holding step at 300 °C might induce a decrease in the capping ability of PVP and the resultant coalescence between neighboring NPs at temperatures higher than the melting point of Bi.

The TEM images of the as-synthesized particles are shown in Fig. 7. The image of Fig. 7b shows the presence of PVP around the particles. The SAED pattern in Fig. 7b indicates the formation of major Bi phase and minor Bi_2O_3 phase. Considering the XRD results of Fig. 3, the minor oxide phase seems to be formed during the sample preparation for TEM analysis. A diffuse and broad ring pattern is also observed in the SAED pattern, indicating the formation of an amorphous phase. The HRTEM image in Fig. 7c shows the formation of an amorphous shell surrounding a Bi crystalline core. The amorphous shell can be formed during the rapid cooling. Rapid cooling induces a sudden drop in solubility of Bi ions. The drop can accelerate the formation of an amorphous shell structure on the preformed crystalline core through heterogeneous nucleation of precipitated Bi atoms.

To confirm the abovementioned synthesis mechanism, Bi NPs were synthesized with different initial precursor concentrations.

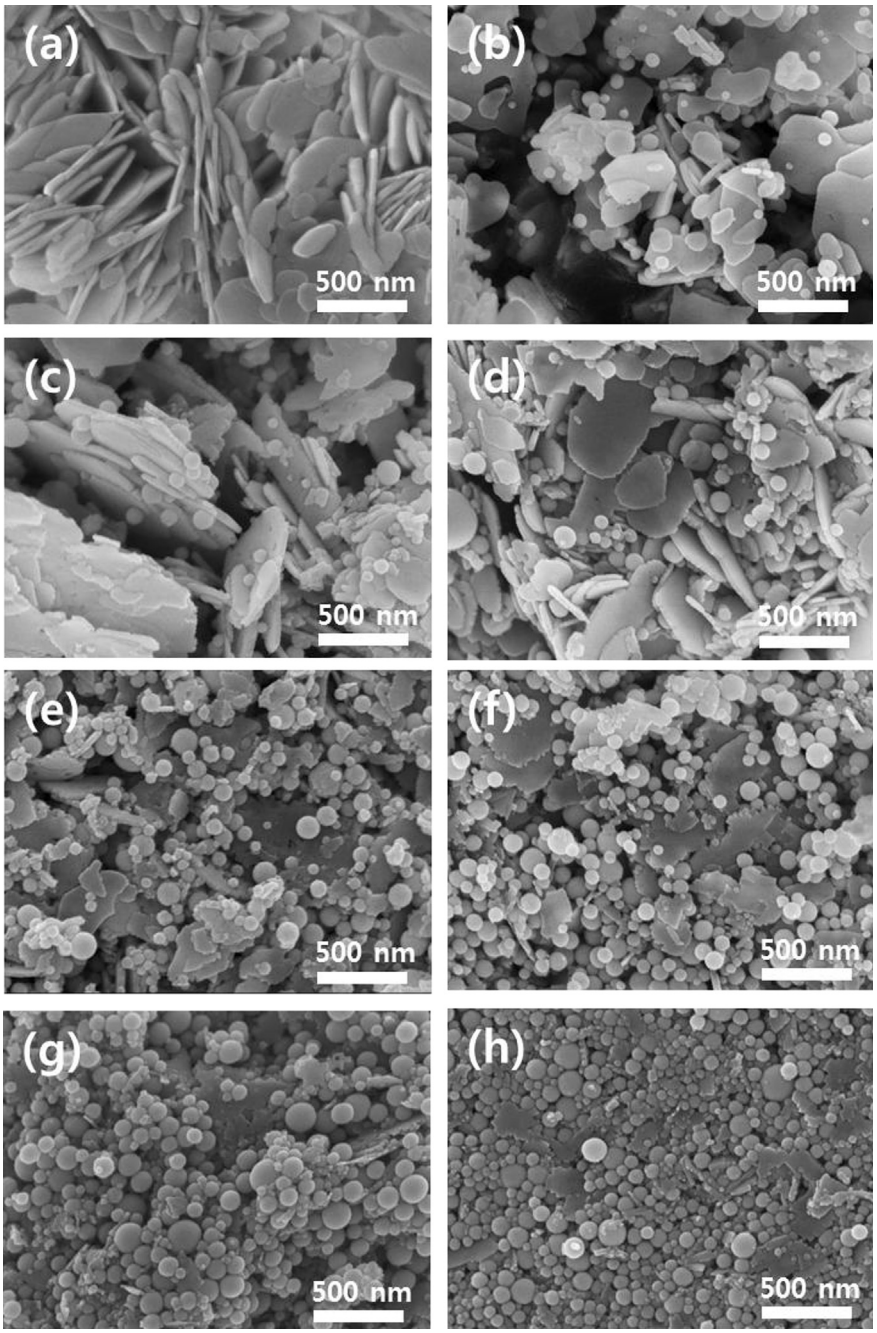

Fig. 2. SEM image showing reduction procedure of Bi(III) subcarbonate to Bi NPs with increasing temperature: after maintaining (a) at 200 °C for 60 min and at (b) 240, (c) 250, (d) 260, (e) 270, (f) 280, (g) 290, and (h) at 300 °C for 5 min.

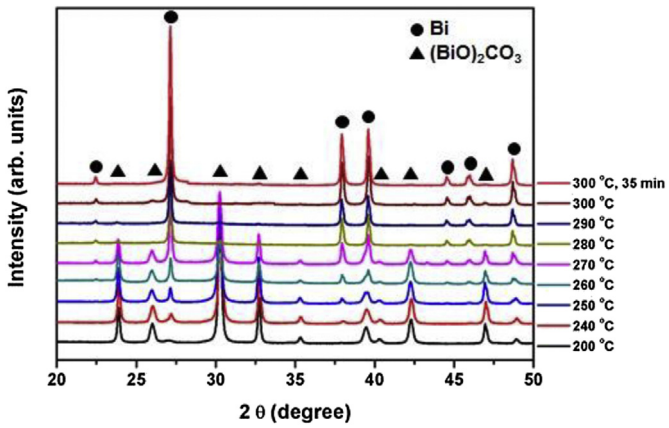

Fig. 3. XRD patterns indicating the reduction procedure of Bi(III) subcarbonate with increasing temperature.

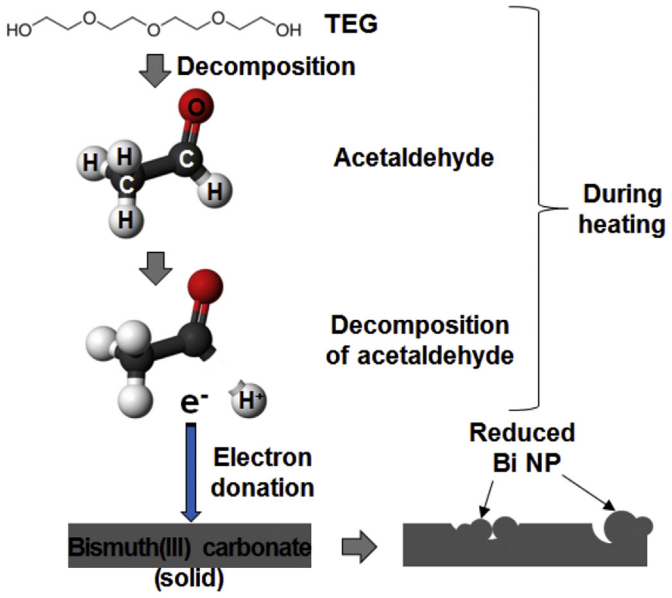

Fig. 5. Schematic showing synthesis mechanism of Bi NPs observed in this study.

Fig. 8 shows SEM images of Bi NPs synthesized with different initial precursor concentrations. The synthesis procedure, including a holding of 35 min at 300 °C, was identical to that typically used. All the synthesized Bi NPs exhibited a spherical shape with initial Bi(III) subcarbonate concentrations of 10–50 mM. However, the synthesized Bi NPs exhibited slightly different particle size distributions.

Fig. 9 shows the average particle size and standard deviation of Bi NPs synthesized with different initial concentrations of Bi(III) subcarbonate. Although the concentration of the Bi(III) subcarbonate precursor varied from 10 mM to 50 mM, only a slight deviation (maximum deviation: 5.8%) in the average particle size was observed. Moreover, the standard deviation observed for each concentration was minimal. The increase in the concentration of the precursor (or metal ions) induces a notable increase of average particle size in the general synthesis of NPs using the reduction of metal ions by wet chemical methods [9]. Thus, the results shown in Fig. 9 could be considered evidence of the direct reduction mechanism from Bi(III) subcarbonate particles to Bi NPs.

To investigate the effect of preheating temperature, the particle size distribution of Bi NPs gathered after the holding step of 35 min at 300 °C was observed as a function of preheating

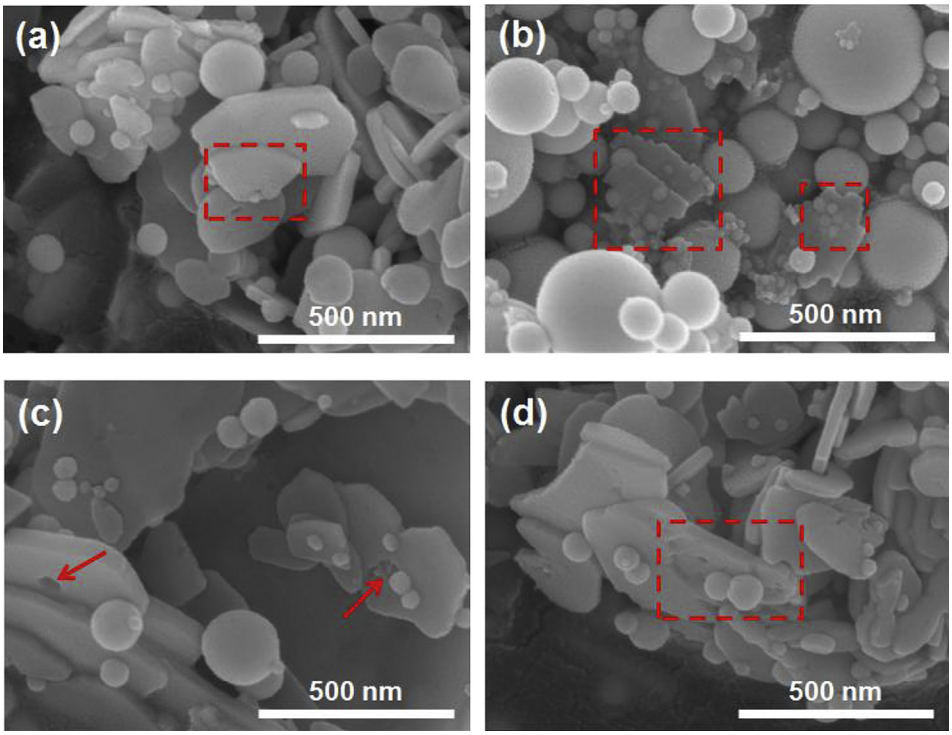

Fig. 4. SEM images showing Bi NPs as-synthesized on platelet Bi(III) subcarbonate: (a) formation of Bi NPs on the edge of a Bi(III) subcarbonate, (b) formation of Bi NPs on the basal plane and edge of a Bi(III) subcarbonate, (c) hole formed in a Bi(III) subcarbonate, and (d) concave face formed in a Bi(III) subcarbonate.

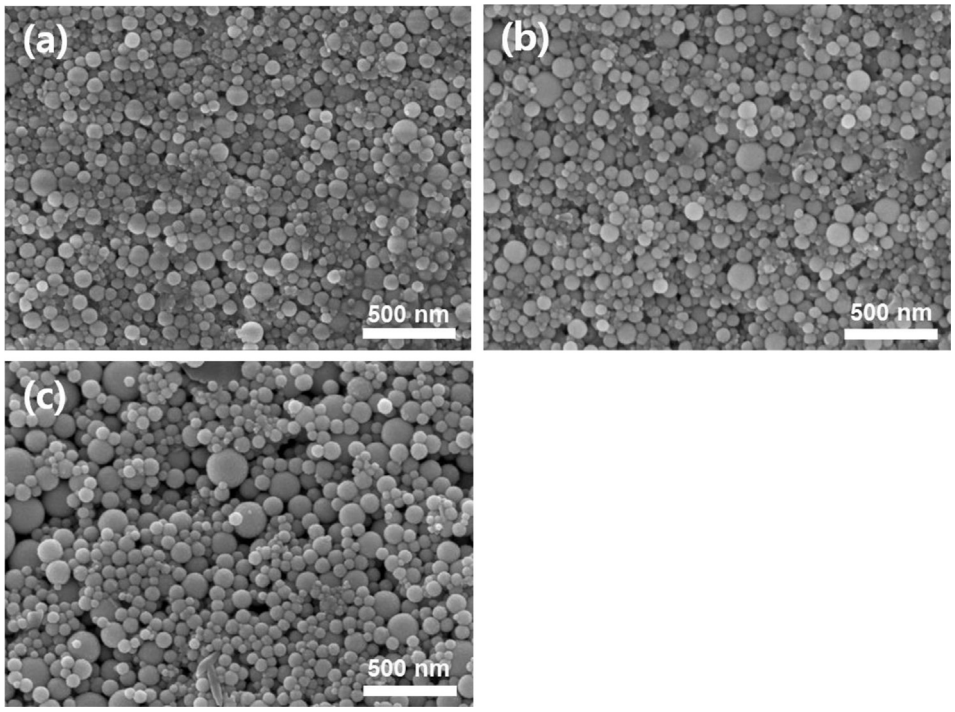

Fig. 6. SEM images of Bi NPs synthesized with different holding times at 300 °C: (a) 35, (b) 40, and (c) 60 min.

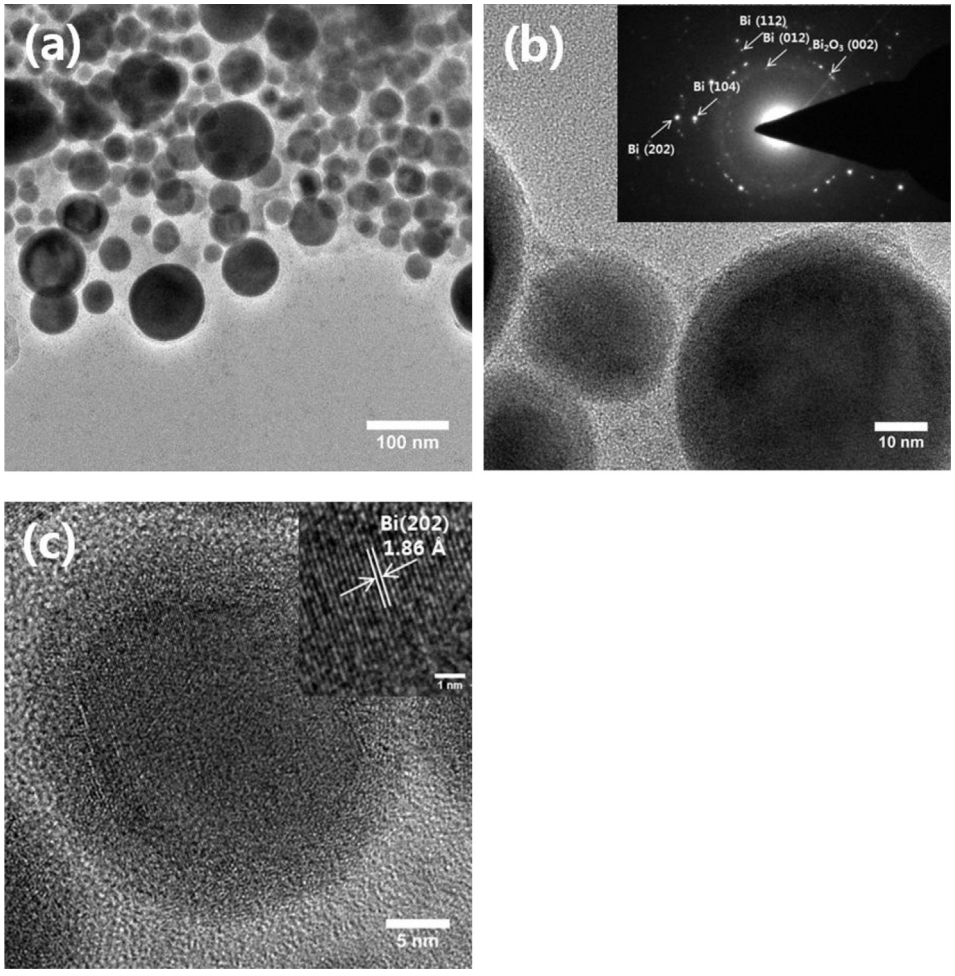

Fig. 7. TEM images of as-synthesized particles at different magnification: (a) average diameter of particles was ~60 nm; (b) presence of PVP around the particles was observed and SAED pattern indicated the formation of major Bi phase and minor Bi_2O_3 phase; (c) HRTEM image showed the formation of an amorphous shell surrounding a Bi core.

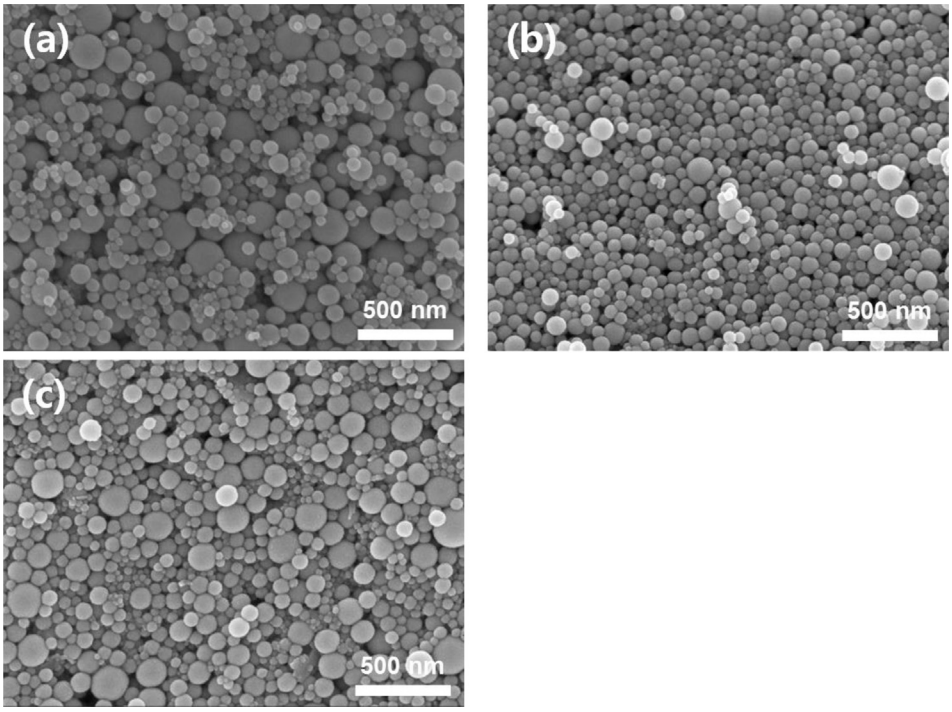

Fig. 8. SEM images of Bi NPs synthesized with different initial Bi(III) subcarbonate concentrations: (a) 10, (b) 25, and (c) 50 mM.

temperature. Fig. 10 shows SEM images of Bi NPs synthesized with different preheating temperatures. As can be seen, the preheating temperature influenced the final size distribution of the Bi NPs. The average particle size and standard deviation of Bi NPs synthesized with different preheating temperatures are summarized in Fig. 11. The Bi NPs preheated at 160 °C showed similar average particle sizes and a greater standard deviation in comparison with the standard sample preheated at 200 °C. Furthermore, the average particle size and standard deviation increased as the preheating temperature increased to 240 °C and 270 °C, resulting in a maximum deviation in average size of 11.8%. The increase in the standard deviation was more obtrusive with increasing preheating temperature. The preheating temperature in this study affected the subsequent heating process. In other words, the preheating at 160 °C might lead to a temperature imbalance in the synthesis medium during the subsequent heating process to 300 °C as compared with the preheating at 200 °C. The temperature imbalance induces local synthesis of Bi NPs, in that some synthesize faster while others are slower, resulting in an increased deviation in size of the Bi NPs. Meanwhile, preheating at temperatures higher than 200 °C will generate more Bi NPs during the holding period of 1 h. The increased peaks of the Bi phase in the XRD results of Fig. 3 show that after heating to 240 °C and especially to 270 °C, more Bi NPs are synthesized and the greater the probability of coalescence between neighboring NPs during the subsequent heating step. The Bi NPs that are finally synthesized from the Bi(III) subcarbonate platelets after the burst formation of Bi NPs at the higher preheating temperature might be relatively small. This consideration explains the increase of size and standard deviation shown in Fig. 11.

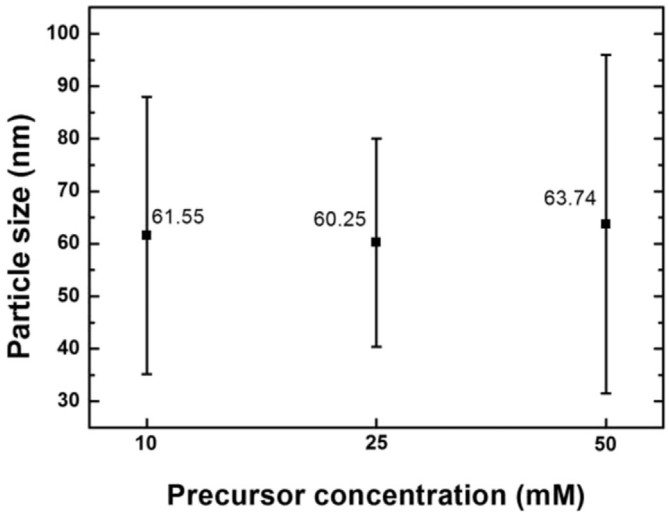

Fig. 9. Average particle size and standard deviation of Bi NPs synthesized with different initial Bi(III) subcarbonate concentrations.

4. Conclusion

Synthesis of spherical Bi NPs was implemented by a novel polyol method using insoluble solid Bi(III) subcarbonate particles. The Bi(III) subcarbonate precursor was directly reduced and gradually transformed to Bi NPs from 240 °C with an increase of temperature during a two-step heating process to 300 °C. The reduced spherical Bi NPs grew from the edge or basal surfaces of the plate-like Bi(III) subcarbonate particles. The electrons participating in reducing the precursor to Bi NPs were supplied from acetaldehyde, a decomposed product of TEG, to the surface of the Bi(III) subcarbonate. Although some Bi(III) subcarbonate platelets were not transformed completely to Bi NPs even after heating to 300 °C, complete removal of the Bi(III) subcarbonate and the enhanced sphericity of the synthesized Bi NPs were accomplished with a holding step at the target temperature for

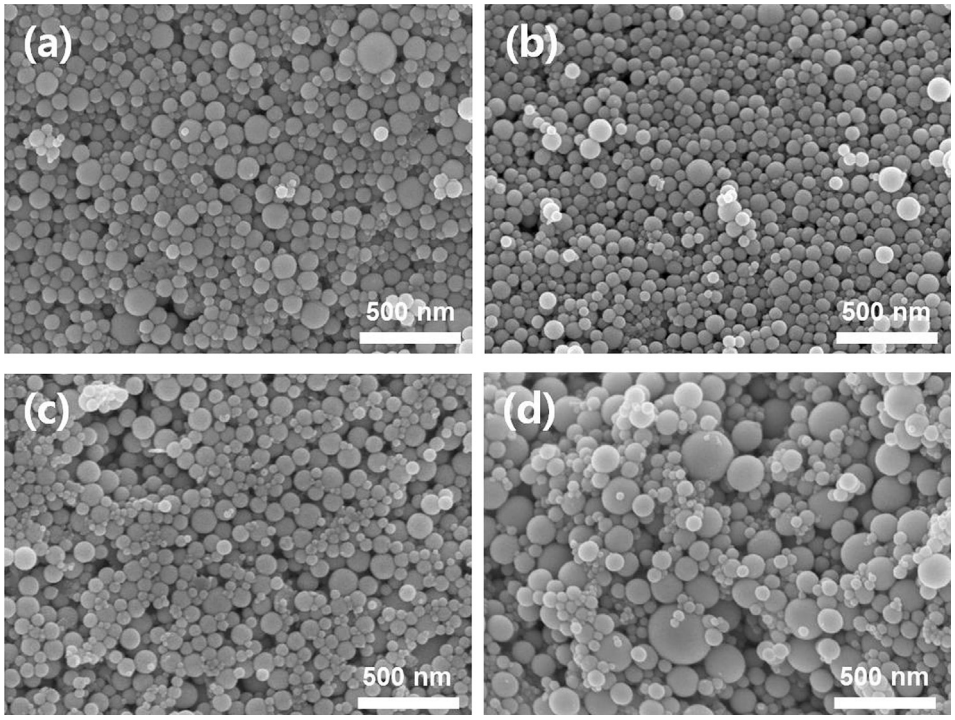

Fig. 10. SEM images of Bi NPs synthesized with different preheating temperatures: (a) 160, (b) 200, (c) 240, and (d) 270 °C.

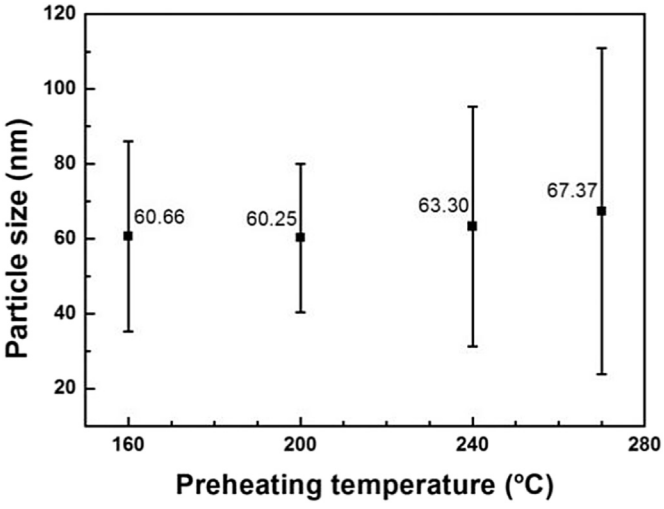

Fig. 11. Average particle size and standard deviation of Bi NPs synthesized with different preheating temperatures.

35 min. The Bi NPs synthesized under optimized conditions that included preheating at 200 °C for 1 h had an average diameter of approximately 60 nm and exhibited excellent sphericity and dispersity.

Acknowledgments

The authors thank Korean Basic Science Institute (KBSI) for the HRTEM, SEM and XRD analyses.

References

[1] C. Goia, E. Matijevic, D.V. Goia, J. Mater. Res. 20 (2005) 1507.
[2] W.J. Tomlinson, I. Collier, J. Mater. Sci. 22 (1987) 1835.
[3] Z. Xia, Z. Chen, Y. Shi, N. Mu, N. Sun, J. Electron. Mater. 31 (2002) 564.
[4] M. Nahacandi, M.A.A. Hanim, Z.N. Ismarrubie, A. Hajalilou, R. Rohaizuan, M.Z.S. Fadzli, J. Electron. Mater. 43 (2014) 579.
[5] Y. Wang, M. Ibisate, Q.Y. Li, Y. Xia, Adv. Mater. 18 (2006) 471.
[6] R.T. Delves, A.E. Bowley, D.W. Hazelden, H.J. Goldsmid, Proc. Phys. Soc. 78 (1961) 838.
[7] G. Cheng, J. Wu, F. Xiao, H. Yu, Z. Lu, X. Yu, R. Chen, Mater. Lett. 63 (2009) 2239.
[8] W.Z. Wang, B. Poudel, Y. Ma, Z.F. Ren, J. Phys. Chem. B 110 (2006) 25702.
[9] Y. Wang, Y. Xia, Nano Lett. 4 (2004) 2047.
[10] U. Jeong, Y. Wang, M. Ibisate, Y. Xia, Adv. Funct. Mater. 15 (2005) 1907.
[11] C.C. Mayorga-Martinez, M. Cadevall, M. Guix, J. Ros, A. Merkoci, Biosens. Bioelectron. 40 (2013) 57.
[12] J.H. Kim, J.H. Lee, Appl. Mech. Mater. 249–250 (2013) 945.
[13] F. Fievet, J.P. Lagier, B. Blin, B. Beaudoin, M. Figlarz, Solid State Ion. 32–33 (1989) 198.
[14] F. Fievet, J.P. Lagier, M. Figlarz, MRS Bull. 14 (1989) 29.
[15] D. Larcher, R. Patrice, J. Solid State Chem. 154 (2000) 405.
[16] M. Tsuji, S. Hikino, M. Matsunaga, Y. Sano, T. Hashizume, H. Kawazumi, Mater. Lett. 64 (2010) 1973.
[17] Y.K. Du, P. Yang, Z.G. Mou, N.P. Hua, L. Jiang, J. Appl. Polym. Sci. 99 (2006) 23.
[18] M.F. Silva, C.A. Da Silva, F.C. Fogo, E.A.G. Pineda, A.A.W. Hechenleitner, J. Therm. Anal. Calorim. 79 (2005) 367.